Soria-Verdugo, Antonio; Goos, Elke; Morato-Godino, Andrés; García-Hernando, Nestor; Riedel, Uwe. (2017). Pyrolysis of biofuels of the future: Sewage sludge and microalgae-Thermogravimetric analysis and modelling of the pyrolysis under different temperature conditions, *Energy Conversion and Management*, v. 138, pp.: 261-272.

DOI: https://doi.org/10.1016/j.enconman.2017.01.059

Pyrolysis of biofuels of the future: sewage sludge and microalgae - Thermogravimetric analysis and modelling of the pyrolysis under different temperature conditions

Antonio Soria-Verdugo[a]*, Elke Goos[b], Andrés Morato-Godino[a], Nestor García-Hernando[a], Uwe Riedel[b]

[a] *Carlos III University of Madrid (Spain), Energy Systems Engineering Group, Thermal and Fluids Engineering Department. Avda. de la Universidad 30, 28911 Leganés (Madrid, Spain).*

[b] *Deutsches Zentrum für Luft- und Raumfahrt e.V. (DLR, German Aerospace Center), Institute of Combustion Technology, Pfaffenwaldring 38-40, 70569 Stuttgart (Germany).*

** corresponding author: asoria@ing.uc3m.es Tel: +34916248465 Fax: +34916249430.*

Abstract

The pyrolysis process of both microalgae and sewage sludge was investigated separately, by means of non-isothermal thermogravimetric analysis. The Distributed Activation Energy Model (DAEM) was employed to obtain the pyrolysis kinetic parameters of the samples, i.e. the activation energy E_a and the pre-exponential factor k_0. Nine different pyrolysis tests at different constant heating rates were conducted for each sample in a thermogravimetric analyzer (TGA) to obtain accurate values of the pyrolysis kinetic parameters when applying DAEM. The accurate values of the activation energy and the pre-exponential factor that characterize the pyrolysis reaction of *Chlorella vulgaris* and sewage sludge were reported, together with their associated uncertainties. The activation energy and pre-exponential factor for the *C. vulgaris* vary between 150 - 250 kJ/mol and 10^{10} - 10^{15} s^{-1} respectively, whereas values ranging from 200 to 400 kJ/mol were obtained for the sewage sludge activation energy, and from 10^{15} to 10^{25} s^{-1} for its pre-exponential factor. These values of E_a and k_0 were employed to estimate the evolution of the reacted fraction with temperature during the pyrolysis of the samples under exponential and parabolic temperature increases, more typical for the pyrolysis reaction of fuel particles in industrial reactors. The estimations of the relation between the reacted fraction and the temperature for exponential and parabolic temperature increases were found to be in good agreement with the experimental values measured in the TGA for both the microalgae and the sludge samples. Therefore, the values reported in this work for the activation energy and the pre-exponential factor of the *C. vulgaris* can be employed as reference values in numerical studies of the pyrolysis process of this biofuel since its chemical composition is quite homogeneous. In the case of sewage sludge, due to the heterogeneity of its composition, the results reported for the kinetic parameters of the pyrolysis process can be employed to describe the pyrolysis of sludge with similar composition.

***Keywords*:** Microalgae, Chlorella vulgaris, Sewage Sludge, Distributed Activation Energy Model (DAEM), Biomass pyrolysis, Thermal Gravimetric Analysis (TGA).

Nomenclature:

a	Heating rate [K min^{-1}].
A_p	Surface of a fuel particle [m^2].
b	Constant for the parabolic temperature profile [ºC min^{-2}].
Bi	Biot number [-].
c	Constant for the exponential temperature profile [min^{-1}].
c_p	Specific heat of the fuel particle [J $kg\ K^{-1}$].
E_a	Activation energy [kJ mol^{-1}].
$f(E)$	Probability density function of the activation energy [-].
h	Convective coefficient [W $m^{-2}\ K^{-1}$].
k	Reaction rate coefficient [s^{-1}].
k_f	Fuel particle thermal conductivity [W $m^{-1}\ K^{-1}$].
k_0	Pre-exponential factor [s^{-1}].
R	Universal gas constant [J $mol^{-1}K^{-1}$].
t	Time [s].
T	Temperature [ºC].
T_p	Fuel particle temperature [ºC].
T_0	Initial temperature of the fuel particle [ºC].
T_∞	Temperature of the surrounding of the fuel particle inside a reactor [ºC].
V	Volatile mass loss [%].
V^*	Volatile mass content [%].
V/V^*	Reacted fraction [%].
V_p	Fuel particle volume [m^3].
ϕ	ϕ function [-].
ρ_p	Fuel particle density [kg m^{-3}].

1. Introduction

A continuous growth of the world population has occurred during the last 50 years, resulting in an increase of the primary energy consumption. Currently, more than 80% of the total primary energy consumption is based on fossil fuels, which are responsible for more than 98% of the carbon dioxide emissions to the

atmosphere, causing the current global warming problems [1]. Therefore, there is a need to evaluate the potential of different alternative fuels capable of substituting fossil fuels, with lower associated pollutant emissions. Two of the most promising alternative fuels, due to entirely different reasons, are sewage sludge and microalgae.

Sewage sludge is the residue produced during the treatment of industrial or municipal wastewater. The main ways of the disposing of sewage sludge nowadays can be divided into three applications: landfill, agricultural use and incineration or thermochemical conversion [2]. Nevertheless, the European regulations try to limit the amount of sewage sludge employed for landfill. Concerning the agricultural use, sewage sludge contains organic matter, nitrogen, and phosphorus, making them suitable as a fertilizer. However, the sludge may also concentrate heavy metals and pathogens, which could cause significant environmental problems. In contrast, the thermochemical conversion of sewage sludge [3] presents several benefits, such as the possibility to recover energy [4], the reduction of the residue volume by 70% and the thermal destruction of pathogens [5]. Furthermore, the population growth in urban areas causes also the problem of an increase in the sewage sludge production. Therefore, the thermochemical conversion of sewage sludge with energy recovery might solve the issue of the increase in residues produced due to the population growth, contributing to a reduction of the dependence on fossil fuels.

Among the potential replacement for fossil fuels, biodiesel is gaining importance in applications such as transport, where other possible substitute fuels count on a limited applicability. The production of biodiesel has been based on different crops, causing social problems as the dilemma regarding the risk of diverting farmland or crops for biofuels production to the detriment of the food supply. The so-called third generation biofuel obtained from microalgae can deal with these social problems since microalgae can be cultivated in freshwater, marine seawater or even wastewater [5]. Microalgae have higher photosynthesis efficiency than energy crops based on terrestrial lignocellulosic biomass, which would help to reduce the concentration of CO_2 in the atmosphere at a faster rate [7]. Besides, microalgae are the fastest-growing photosynthesizing organisms, being able to complete an entire growing cycle in few days [1]. There is a large number of species of microalgae, among them the most widely grown is *Chlorella vulgaris* [8].

In comparison to other thermochemical conversion processes, such as combustion or gasification, pyrolysis presents the advantage of producing mainly an easy to store and transport liquid product, in particular for those fuels characterized by high volatile matter and low fixed carbon content, like sewage sludge and microalgae [9]. Pyrolysis was found to be the optimal thermochemical process for sewage sludge by [10], due to its favorable energy balance, material recovery, and zero-waste conversion. Several methods have been employed in the literature to model the pyrolysis process of biomass, such as the single step model

[11], the two parallel reaction model [12], the three pseudo-components model [13], the sectional approach model [14], or the Distributed Activation Energy Model (DAEM) [15]. [16] and [17] proposed a simplification for DAEM to easily obtain the activation energy and the pre-exponential factor of a sample from different thermogravimetric analysis (TGA) tests. This simplified DAEM has been employed, achieving a proper agreement with experimental measurements, for a wide variety of samples, such as coal [18], charcoal [19], polymers [20], oil shale [21], medical waste [22], sewage sludge [23], microalgae [24, 25], and several different types of biomass [26, 27, 28, 29, 30, 31].

In this work, the pyrolysis of the *C. vulgaris* microalgae and sewage sludge are investigated separately, by means of non-isothermal thermogravimetric analysis. Independent TGA tests of both biomasses under different constant heating rates were conducted and the experimental results were employed as input data to apply the Distributed Activation Energy Model. Nine different TGA curves were employed for both the *C. vulgaris* and the sewage sludge samples in order to obtain accurate values of pyrolysis kinetic parameters, i.e. the activation energy and the pre-exponential factor, of the samples when applying DAEM [32]. The accurate values of the kinetic parameters of the pyrolysis reactions of *C. vulgaris* and sewage sludge are reported together with their associated uncertainties. Finally, the values of the activation energy and pre-exponential factor of the samples were employed to simulate the evolution of the pyrolysis process of the biomasses under exponential and parabolic temperature increases, more typical of the pyrolysis process of fuel particles in industrial reactors. The comparison of the numerical results with experimental measurements carried out in the TGA resulted in an excellent agreement.

2. Mathematical model

The simplified Distributed Activation Energy Model was applied to obtain accurate values of the activation energy E_a and the pre-exponential factor k_0 of *C. vulgaris* and sewage sludge kinetics of pyrolysis. The activation energy is the energy needed to activate the pyrolysis reactions and the pre-exponential factor expresses the empirical temperature dependence of the reaction rate coefficient k [33].

DAEM considers a complex fuel as a mixture of components, which decompose following first-order reactions. Thus, a large number of independent irreversible first-order reactions occur simultaneously with different associated activation energies. The reacted fraction V/V^* in a pyrolysis reaction can be determined as [16]:

$$1-\frac{V}{V*}=\int_0^{\infty}\exp\left(-k_0\int_0^t e^{-E/RT}dt\right)f\left(E\right)\cdot dE\ . \tag{1}$$

where V is the volatile matter content released at time t, V^* is the total volatile matter content of the sample, k_0 is the pre-exponential factor corresponding to the activation energy E, R is the universal gas constant, and $f(E)$ is the probability density function of the activation energy. The exponential term in Eq. (1) is the so-called ϕ function:

$$\phi(E,T) = \exp\left(-k_0 \int_0^t e^{-E/RT} dt\right) \tag{2}$$

which is typically approximated by a step function at a value of the activation energy $E = E_a$, obtaining for the reacted fraction:

$$\frac{V}{V^*} = 1 - \int_{E_a}^{\infty} f(E) \cdot dE = \int_0^{E_a} f(E) \cdot dE \ . \tag{3}$$

[16] proposed a value for $\phi(E_a,T) = 0.58$, which has been employed for several different types of mineral carbon and biomass samples obtaining good agreement with experimental measurements. Approximating the integral in the ϕ function, for a constant heating rate a, to:

$$\phi(E,T) = \exp\left(-\frac{k_0}{a} \int_0^T e^{-E/RT} dT\right) \approx \exp\left(-\frac{k_0 R T^2}{aE} e^{-E/RT}\right) \tag{4}$$

and using the value proposed by [16] for $\phi(E_a,T) = 0.58$, the widely used Arrhenius equation for the pyrolysis of a sample under a constant heating rate a can be derived:

$$\ln\left(\frac{a}{T^2}\right) = \ln\left(\frac{k_0 R}{E_a}\right) + 0.6075 - \frac{E_a}{R}\frac{1}{T} \ . \tag{5}$$

Based on this Arrhenius equation, [17] proposed a method to determine the activation energy E_a and the pre-exponential factor k_0 of a sample from TGA curves of the pyrolysis process obtained for different heating rates a.

3. Experimental Measurements

The pyrolysis tests were performed in a thermogravimetric analyzer TGA Q500 from TA Instruments. A nitrogen flowrate of 60 ml/min was supplied to the furnace to guarantee the existence of an inert atmosphere. The temperature profile programmed to the TGA consisted of two processes occurring in series, first a drying process of the sample at 105 ºC and then the pyrolysis process taking place when increasing the temperature of the sample in the inert atmosphere up to 800 ºC. For the pyrolysis tests conducted to determine the kinetic parameters of the pyrolysis, a constant heating rate was used, and for a

147 more industrial application, a series of consecutive constant heating rates obtaining exponential or parabolic
148 temperature increases, as described in [34], were employed. For the pyrolysis measurements at constant
149 heating rates, nine different tests were carried out, as proposed by [32], using heating rates of 10, 13, 16,
150 19, 22, 25, 30, 35, 40 K/min. These heating rates are low compared to industrial applications, nevertheless
151 similar results were obtained by [31] when applying DAEM to TGA curves obtained at higher heating rates,
152 up to 200 K/min.

153 The sensitivity of the TGA mass measurement is 0.1 μg and the weighing precision is ±0.01%. The dynamic
154 baseline drift during a heating process of an empty platinum pan from 50 ºC to 1000 ºC at 20 K/min is lower
155 than 50 μg with no baseline subtraction. The TGA temperature accuracy during an isothermal process is
156 ±1 ºC and the temperature precision is ±0.1 ºC. A mass of 10.0±0.5 mg of the sample, sieved previously
157 under 100 μm, was employed in the pyrolysis measurements in the TGA to reduce heat transfer effects in
158 the sample [26, 35]. Each pyrolysis test was conducted three times to guarantee the repeatability of the
159 process (obtaining differences lower than 1 %), and a blank experiment was also run for each heating rate to
160 exclude buoyancy effects.

161 The mono-cellular green microalgae *C. Vulgaris* have a diameter of 4-10 μm and a spherical form. They
162 grow in flowing or standing fresh and brackish water and contain as dried samples around 50% of proteins
163 and a high amount of a multitude of unsaturated fatty acids, such as alpha-linolenic acid and carotenoids, as
164 lutein. Additionally, they contain minerals with iron, calcium, magnesium, zinc, potassium, manganese and
165 sulfur. The *C. vulgaris* microalgae samples employed for the study were cultivated and dried by the
166 company AlgaEnergy S.A. in 2016 in Madrid.

167 The sludge was obtained from the municipal sewage treatment plant of Loeches (Madrid, Spain) in February
168 2016. The sludge was taken after the pre-drying process at 80 ºC in a fluidized bed in the sewage treatment
169 plant. This sewage sludge sample is quite different to that investigated earlier [23], which was obtained from
170 the municipal sewage treatment plant of La China (Madrid, Spain) in 2012.

171 The samples of *C. Vulgaris* and sewage sludge were characterized by proximate and elemental analyses.
172 The proximate analysis was performed in the TGA Q500 from TA Instruments to determine the moisture,
173 ash, volatile matter, and fixed carbon contents of the samples. The moisture content was characterized as
174 the mass released by the sample at 105 ºC. The ash content was determined as the percentage of mass
175 remaining after a heating of the sample up to 550 ºC, supplying the furnace with an oxygen flow rate of 60
176 ml/min using a heating rate of 10 K/min, and an isothermal process at 550 ºC until the mass of the sample
177 stabilized. The volatile matter content of the samples was measured as the percentage of mass released by

the sample during a heating process at a heating rate of 10 K/min from 105 ºC to 900 ºC and an isothermal process at 900 ºC in an inert atmosphere which was obtained introducing a flux of 60 ml/min of nitrogen in the furnace, until the mass of the sample stabilized. Finally, the fixed carbon content was obtained from the difference between these two procedures.

The elemental analysis of the sample was carried out in a LECO TruSpec CHN analyzer, where the carbon and hydrogen content of the sample are measured using an infrared absorption detector for the exhaust gases obtained from a complete combustion of the sample. The nitrogen content is determined conducting the exhaust gases through a thermal conductivity cell. The carbon and nitrogen contents are measured with a precision of ±0.5%, while the precision of the measurement of the hydrogen content is ±1%. Heating value tests of the samples were also conducted in an isoperibolic calorimeter Parr 6300 with an instrument precision of 0.10% relative standard deviation. Control limits were based on 99% confidence (3 sigma) values. The calorimeter has a temperature resolution of 0.0001 °C (data obtained from the manufacturer Parr Instruments).

4. Results and Discussion

The results of the chemical, thermogravimetric and kinetic analysis of microalgae and sewage sludge as potential biofuels of the future are shown and discussed in the following sections.

4.1. Physical and chemical properties of Chlorella Vulgaris and Sewage sludge

The results obtained from the proximate analysis, the ultimate analysis and the heating value tests of the microalgae *C. vulgaris* and sewage sludge samples are reported in Table 1.

Table 1: Results obtained from the characterization of the *C. vulgaris* and the sewage sludge samples (d: dry basis, daf: dry ash free basis, * obtained by difference).

Table 1 shows that the volatile matter content of both the *C. vulgaris* and the sewage sludge is high, and therefore the pyrolysis study of these biofuels is justified. Concerning the elemental analysis, the carbon and hydrogen contents of *C. vulgaris* are higher than those of sewage sludge samples, resulting therefore in a higher heating value for the microalgae sample. The nitrogen content of both samples is high, which indicates a high pollution level of NO_x emission if direct combustion of these biomasses is selected as the thermochemical conversion method. Therefore, an appropriate NO_x after-treatment system is necessary to satisfy EU emission regulations. Additionally, the ash content, especially in sewage sludge, needs to be considered as it influences the optimal operation and maintenance conditions of pyrolysis, gasification, and combustion systems for instance through the formation of slag, which affect the heat transfer to the wall [36].

Also ash compounds like heavy metals should not end up in the environment due to their negatively impact on health of humans, animals, plants and microorganism.

The composition of *C. vulgaris* samples from different sources, shown in Table 2, is quite homogeneous.

Table 2: Comparison of characterization results of *C. vulgaris* samples. M: Moisture, V: Volatile matter, A: Ash, FC: Fixed Carbon, C: Carbon, H: Hydrogen, N: Nitrogen, S: Sulfur, O: Oxygen, w: wet, d: dry, daf: dry ash free, * obtained by difference.

As can be seen from Table 3, sewage sludge samples are quite heterogeneous. The reason is that sewage sludge is a complex mixture of water, organic compounds (such as carbohydrates, lipids, and proteins), microorganisms which can be pathogenic before they were destroyed through heating processes, and inorganic substances e.g. silicates and metal containing compounds, which are left over as ash after a high-temperature heating process. The composition of sewage sludge depends strongly on the origin of the wastewater, e.g. industrial, agricultural or rain water and the season, as well as the used pretreatment methods, such as aerobic, anaerobic, chemical or thermal stabilization, dewatering, thickening and drying processes [45]. This influences, for instance, the pyrolysis product distribution as shown by [2] for three samples of anaerobically digested sewage sludge obtained from three different urban wastewater treatment plants.

Table 3: Comparison of characterization results of sewage sludge samples. M: Moisture, V: Volatile matter, A: Ash, FC: Fixed Carbon, C: Carbon, H: Hydrogen, N: Nitrogen, S: Sulfur, O: Oxygen, w: wet, d: dry, daf: dry ash free, * obtained by difference.

4.2. Determination of the kinetic parameters of the pyrolysis

The pyrolysis tests using constant heating rates were conducted under a controlled atmosphere in the thermogravimetric analyzer. The procedure described by [32] was followed to obtain accurate values of the kinetic parameters of the pyrolysis, i.e. the activation energy E_a and the pre-exponential factor k_0. Following this procedure, tests using nine different heating rates (a = 10, 13, 16, 19, 22, 25, 30, 35, 40 K/min) were performed. The evolution of the reacted fraction V/V^*, defined as the percentage of the total volatile matter released by the sample, with temperature T is shown in Figure 1 a) for the *C. vulgaris* and in Figure 1 b) for the sewage sludge sample, up to a temperature of 600 °C. Under a constant nitrogen flow, carbonaceous compounds, measured as fixed carbon amount, volatilize between 500 - 700 °C and the ash melts at temperatures above around 800 °C, which was not investigated in this study.

The pyrolysis of both samples occurred between 150 and 600 ºC, nevertheless the evolution of the reacted fraction of sewage sludge with temperature is more progressive than that of the microalgae sample, for which the pyrolysis takes place faster for temperatures in the range 250 - 450 ºC. Furthermore, the effect of the heating rate variation on the reacted fraction is higher for the *C. vulgaris* sample, obtaining a displacement of the curve to higher temperatures when increasing the heating rate, a typical result for non-isothermal pyrolysis reactions [59, 60]. This effect is slighter for the sewage sludge, resulting in a collapse of the reacted fraction curves for the different heating rates in a narrow zone.

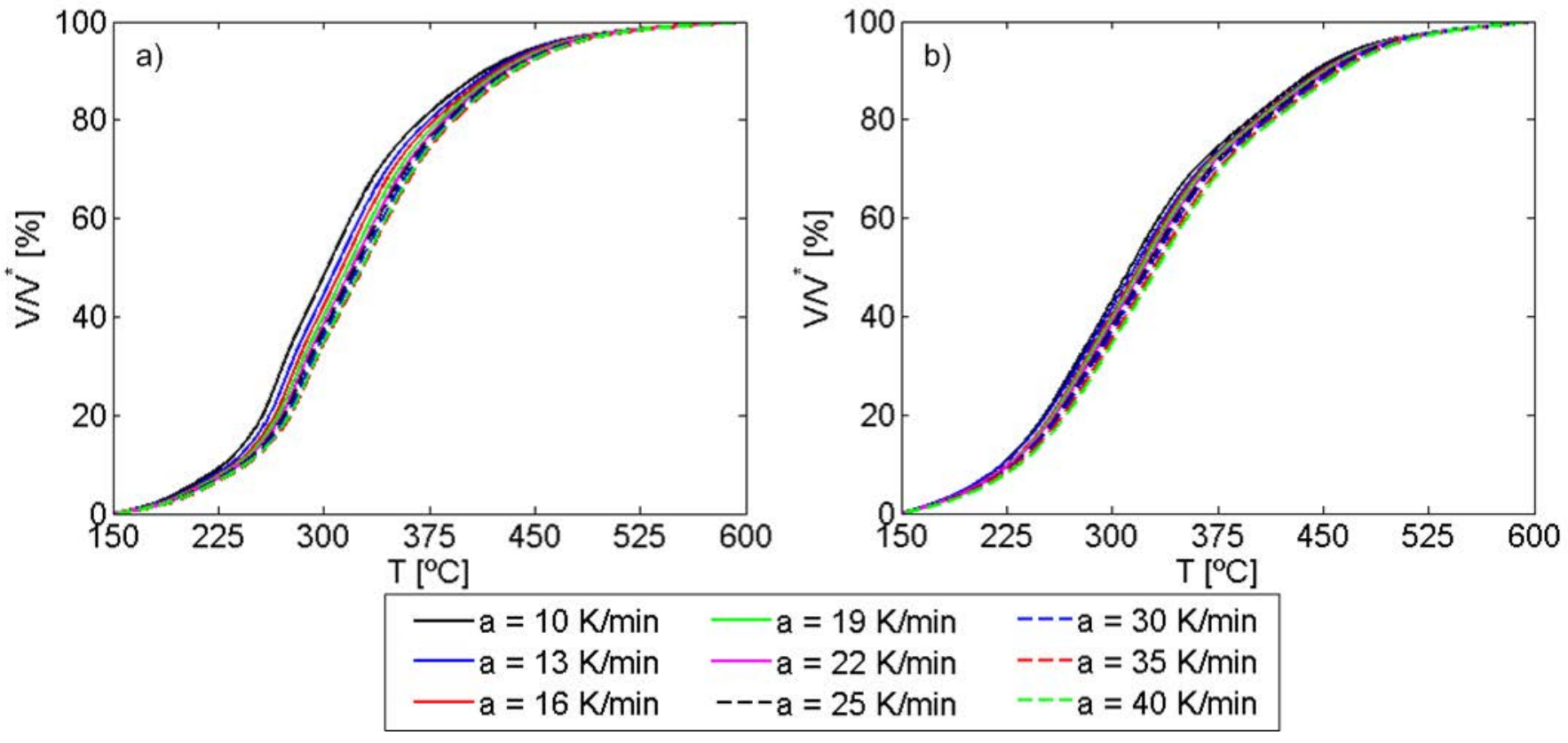

Figure 1: Evolution of the reacted fraction, *V/V**, with temperature, *T*, during the pyrolysis process at constant heating rates. a) *C. vulgaris*, b) Sewage sludge.

From the reacted fraction curves shown in Figure 1, and given the Arrhenius equation (Eq. 5), the Arrhenius plot can be built by plotting $ln(a/T^2)$ as a function of $1/T$ for different values of the reacted fraction V/V^*. Even though all calculations within this paper were carried out using intervals of 1% for the conversion rate, Figure 2 shows the Arrhenius plots of the *C. vulgaris* (a) and the sewage sludge (b), built using conversion rate intervals of 5% to improve data visualization. The Arrhenius plot of sewage sludge is wider because of the more progressive evolution of the reacted fraction with temperature observed in Figure 1 b). The Arrhenius plots can be employed to determine the activation energy E_a and the pre-exponential factor k_0 of the samples by linearizing the points obtained for the different reacted fractions V/V^*. Both for the microalgae and the sludge samples, the points in the Arrhenius plot present a high linearity. To quantify the linearity of the Arrhenius plots, the determination coefficient of the linear fitting of the points, R^2, was calculated. The results can be observed in Figure 3, both for the *C. vulgaris* and the sewage sludge. A high linearity, i.e. high values of R^2, can be observed for a wide range of reacted fractions between 20% and 80%, whereas the

values of the determination coefficient of the fitting decrease for low and high reacted fractions, where the slope of the curve $V/V^*–T$ is smooth, as shown in Figure 1.

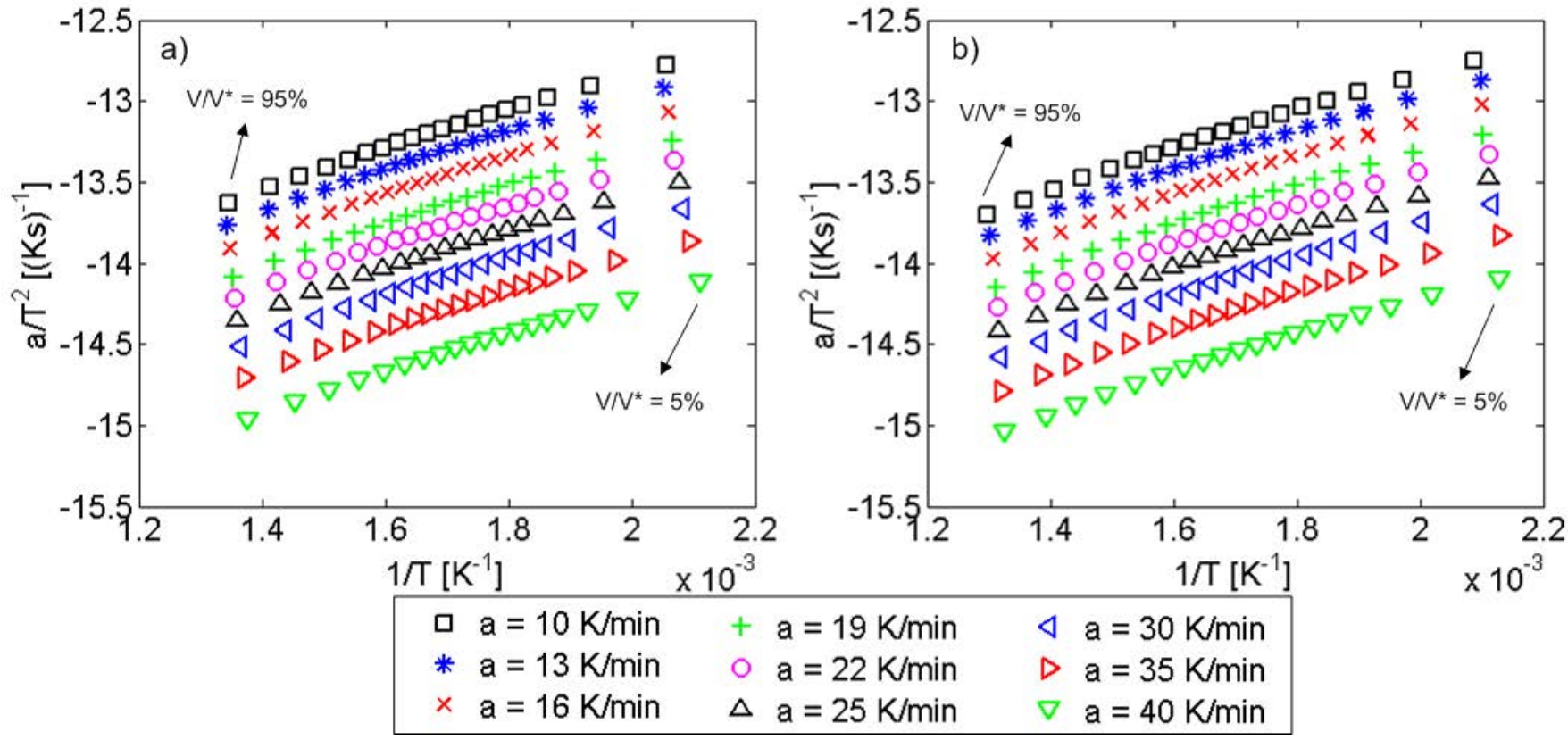

Figure 2: Arrhenius plot obtained using conversion rate intervals of 5%. a) *C. vulgaris*, b) Sewage sludge.

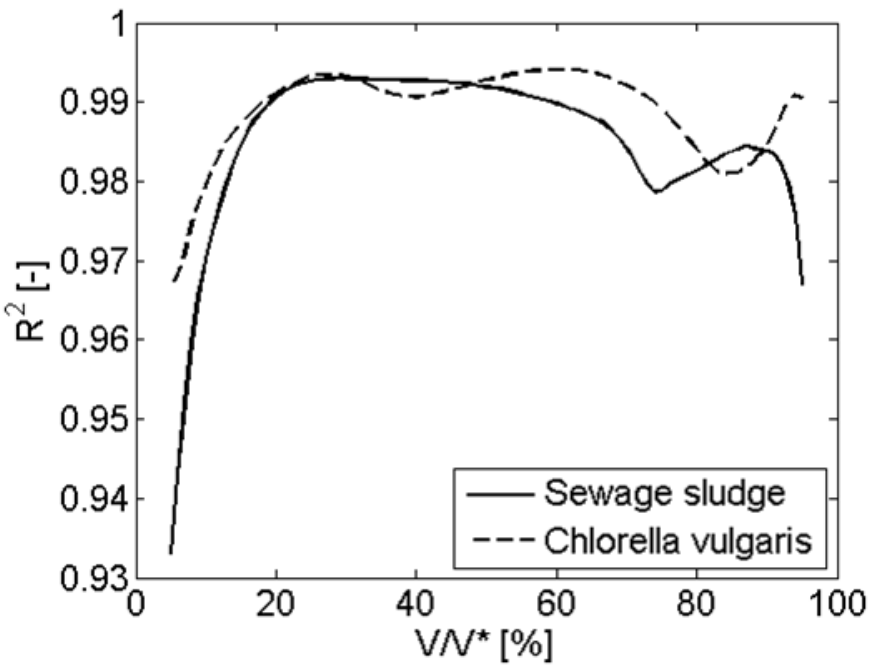

Figure 3: Determination coefficient of the linear fitting of the Arrhenius plot.

Considering the Arrhenius equation for constant heating rates (Eq. 5), the kinetic parameters of the pyrolysis reaction, i.e. the activation energy E_a and the pre-exponential factor k_0, can be obtained for each reacted fraction from the linear fitting of the values of the Arrhenius plot ($ln(a/T^2) = m \cdot (1/T) + n$). Equaling terms of Eq. 5 with the linear fitting, the activation energy E_a and the pre-exponential factor k_0 of the samples can be calculated from the slope m and the intercept n of the linear fitting as:

$$E_a = -m \cdot R \tag{6}$$

$$k_0 = -m \cdot \exp(n - 0.6075) \tag{7}$$

Accurate values of the activation energy E_a and the pre-exponential factor k_0 can be calculated using the nine different reacted fraction curves shown in Figure 1, obtained for different constant heating rates, and considering the uncertainties of the mass, the temperature T and the heating rate a for the linearization of the values of the Arrhenius plot, as stated by [32]. The accurate values of E_a and k_0 for the *C. vulgaris* and the sewage sludge are shown in Figure 4. The activation energy of the *C. vulgaris* varies between around 150 and 250 kJ/mol, while its pre-exponential factor is in the range from 10^{10} to 10^{15} s^{-1}. Similar values for the kinetic parameters of the pyrolysis reaction were obtained for samples of the *Chlorella* microalgae by [44, 38, 61–66], and for different microalgae species such as *Nannochloropsis* oculata and *Tetraselmis sp*. by [24]. In contrast, higher values for both E_a, ranging from 200 and 400 kJ/mol, and k_0, varying between 10^{15} and 10^{25} s^{-1}, were obtained for sewage sludge. These values of the kinetic parameters for sewage sludge are in accordance with the measurements of different authors [58, 67–70]. In a previous work, [23] slightly lower values were obtained for the activation energy and pre-exponential factor of sewage sludge. Nonetheless, it should be noticed that the sewage sludge analyzed in [23] was obtained from a different municipal sewage treatment plant, La China (Madrid, Spain), and were collected in 2012. Furthermore, the values of E_a and k_0 reported in [23] were obtained from just three TGA curves and thus, a higher uncertainty could be expected for these values.

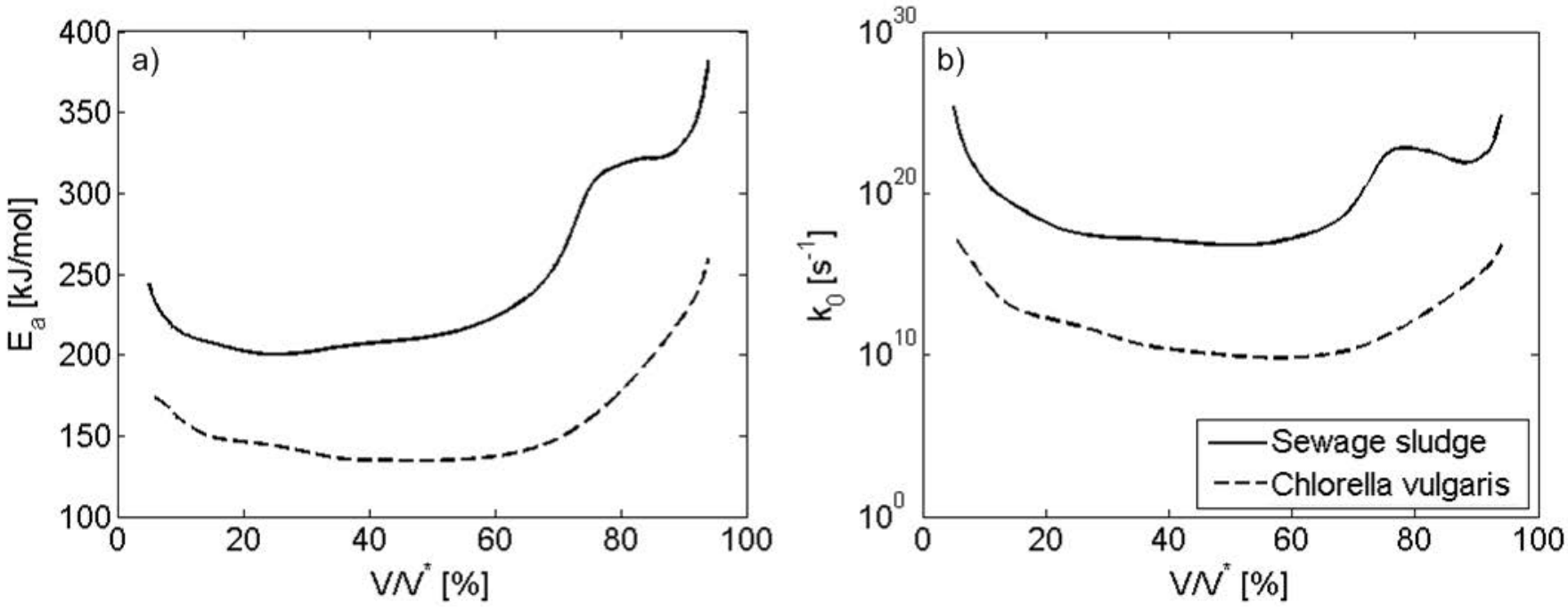

Figure 4: Kinetic parameters of the pyrolysis process: a) activation energy and b) pre-exponential factor.

The absolute and relative uncertainties associated with the kinetic parameters, E_a and k_0, of *C. vulgaris* and sewage sludge are reported in Figure 5. The mathematical procedure to determine the uncertainties associated with the activation energy and the pre-exponential factor is described in detail in [32]. As can be observed, the absolute uncertainties of the activation energy depend on the stage of pyrolysis process and can be as low as 1.35 kJ/mol for the *C. vulgaris* algae and 2.03 kJ/mol for the sewage sludge, respectively. They are, for all the reacted fractions, lower than 2.5 kJ/mol for the *C. vulgaris*, and 4 kJ/mol for sewage

sludge over the whole pyrolysis process, resulting in similar relative uncertainties of less than 1.3% for the activation energy of both samples. Nevertheless, the relative uncertainties for the pre-exponential factor differ, obtaining larger values for sewage sludge, as a result of its higher activation energy, shown in Figure 4 a), which means a higher slope of the linearization that would lead to a higher uncertainty in the intercept of the linearization. For both the *C. vulgaris* and the sewage sludge, the relative uncertainty of the pre-exponential factor is higher for low and high values of the reacted fraction V/V^*, as a consequence of the lower linearity of the Arrhenius plot values in these zones, which can be proved by the lower determination coefficient R^2 obtained for low and high V/V^* (Figure 3). Even though the values of the relative uncertainty of k_0 might seem to be high, the effect of this parameter in the pyrolysis reaction is much lower than that of E_a due to the exponential function (see Eq. 1). Therefore, the values shown in Figure 4 for the activation energy and the pre-exponential factor of the *C. vulgaris* and the sewage sludge are accurate enough for most modelling and optimization purposes and could be employed to model the pyrolysis process of these types of biomass.

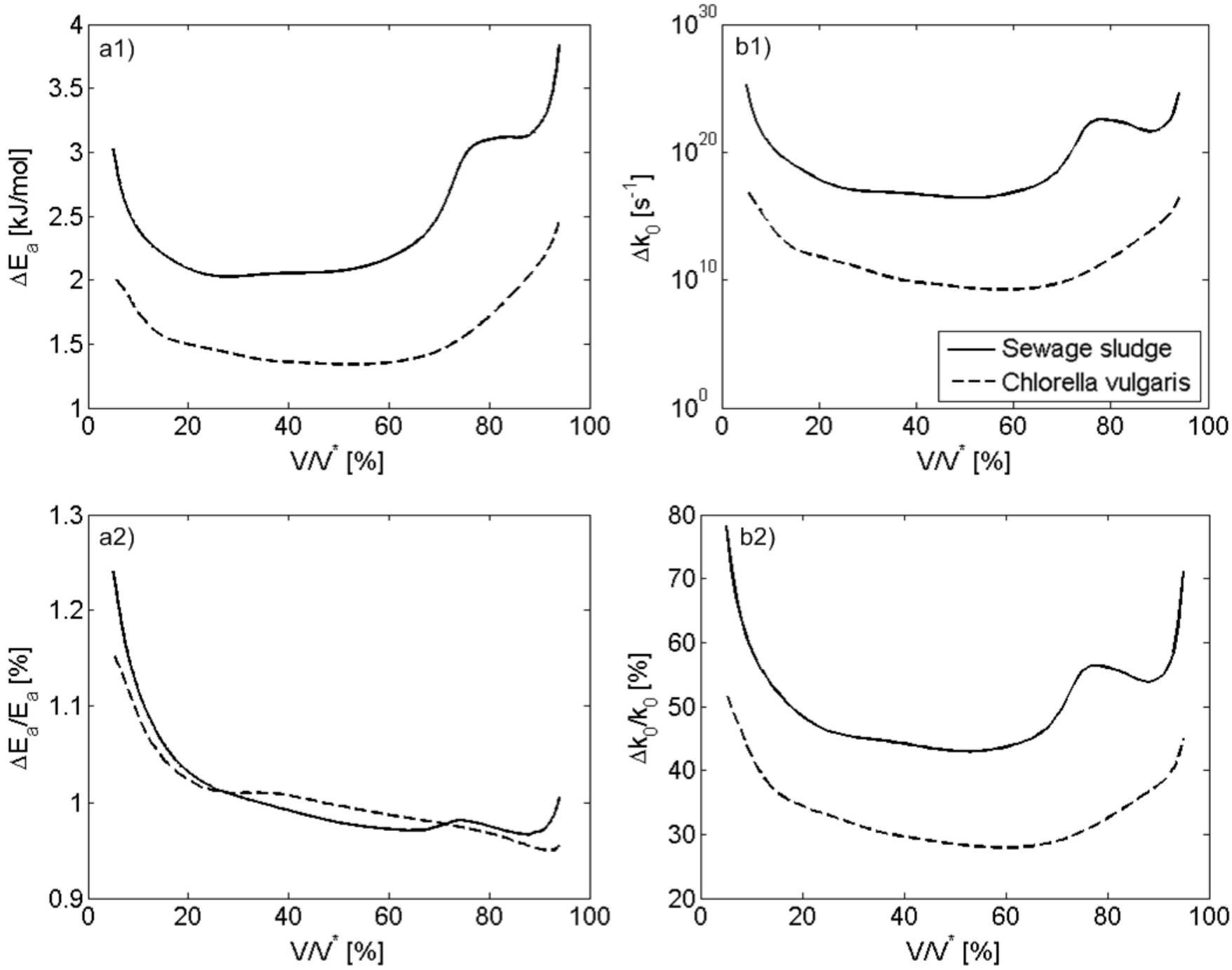

Figure 5: Uncertainties associated with the kinetic parameters of the pyrolysis process: a) activation energy, b) pre-exponential factor, 1) absolute uncertainty, 2) relative uncertainty.

4.3. Validity of the kinetic parameters of pyrolysis for typical temperature increases of fuel particles

The values of the kinetic parameters of the pyrolysis process reported in Figure 4 and their associated uncertainties, shown in Figure 5, correspond to pulverized samples, with particles diameter below 100 μm. However, in industrial applications, the fuels to be pyrolysed are typically larger particles, such as pellets, and thus the temperature inside the fuel particles is subjected to heat transfer effects.

The evolution of the interior temperature of the fuel particles with time is governed by the Biot number, *Bi*, which relates the convective heat transfer between the solid surface and the surrounding with the heat transfer by conduction inside the particle. The Biot number is defined as:

$$Bi = \frac{h \cdot L_c}{k_f}\,, \tag{8}$$

where h is the convective coefficient, L_c is the characteristic length and k_f is the thermal conductivity of the fuel particle. The value of the thermal conductivity is characteristic of the fuel analyzed, however the convective coefficient and the characteristic length could vary in different applications. The convective coefficient can vary depending on the technology employed for the thermochemical conversion process between around 5 and 100 W/m^{2}K. Furthermore, the characteristic length of the fuel may vary from a couple of centimeters for pellet particles to tens or hundreds of micrometers when the fuel is supplied to the reactor as powder. The range of variation of both h and L_c causes a wide range of variation for the Biot number.

When the thermal conduction inside the fuel particle is much faster than the convective heat transfer at the particle surface, i.e. $Bi << 1$, the temperature variation inside the fuel particle can be neglected, assuming that the whole particle is at the surface temperature. In such cases, the Lumped Capacitance Method can be applied to determine the temperature variation inside the particle, equaling the energy increase inside the particle to the heat exchanged by convection on its surface. The result of the Lumped Capacitance Method is an exponential variation of the fuel particle temperature $T_p(t)$ from its initial value T_0 to the temperature of the environment inside the reactor T_∞, in the form:

$$\frac{T_p(t) - T_\infty}{T_0 - T_\infty} = \exp\left[-\frac{h \cdot A_p}{\rho_p \cdot V_p \cdot c_p} t\right] \tag{9}$$

with the surface of a fuel particle A_p, the fuel particle density ρ_p, the fuel particle volume V_p and the specific heat of the fuel particle c_p.

In contrast, when the thermal conduction inside the fuel particle cannot be considered to be much faster than the convective heat transfer at the particle surface, the Lumped Capacitance Method is no longer valid, and the temperature inside the fuel particle differs from that of its surface. In these cases, the temperature distribution inside the fuel particle can be assumed to be parabolic.

Therefore, different tests were conducted in the TGA to characterize the pyrolysis of the *C. vulgaris* and the sewage sludge under exponential and parabolic temperature increases, following the trends of the temperature increases inside the fuel particles in industrial applications. Both the exponential and parabolic temperature increases were obtained in the TGA as a sequence of 25 short constant heating rate increases, as described in [34].

4.4. Exponential temperature increases

The exponential temperature increases tested during the pyrolysis of the samples in the TGA were in the form:

$$T\left[^{\circ}\mathrm{C}\right] = 146.5 + 3.5 \cdot \exp\left(c \cdot t\right). \tag{10}$$

Two different exponential temperature increases were programmed for each sample, varying the value of *c*, $c = 0.023$ min^{-1} and $c = 0.071$ min^{-1}, these being the limit values studied in [34]. The Arrhenius equation derived from the simplified Distributed Activation Energy Model for exponential temperature increases was obtained by [34]:

$$\ln\left(\frac{c}{T}\right) = \ln\left(\frac{k_0 R}{E_a}\right) + 1.7467 - \frac{E_a}{R}\frac{1}{T}. \tag{11}$$

Therefore, Eq. 11 can be solved using the values of the activation energy E_a and the pre-exponential factor k_0 of the sample, shown in Figure 4, to obtain the temperature *T* for each reacted fraction *V/V**. The results obtained solving Eq. 11 are presented in Figure 6 together with the experimental measurements of the pyrolysis process performed in the TGA under exponential temperature increases, for both the *C. vulgaris* and the sewage sludge samples. A proper agreement between the numerical results obtained from Eq. 11 and the experimental measurements can be observed in Figure 6 for both samples.

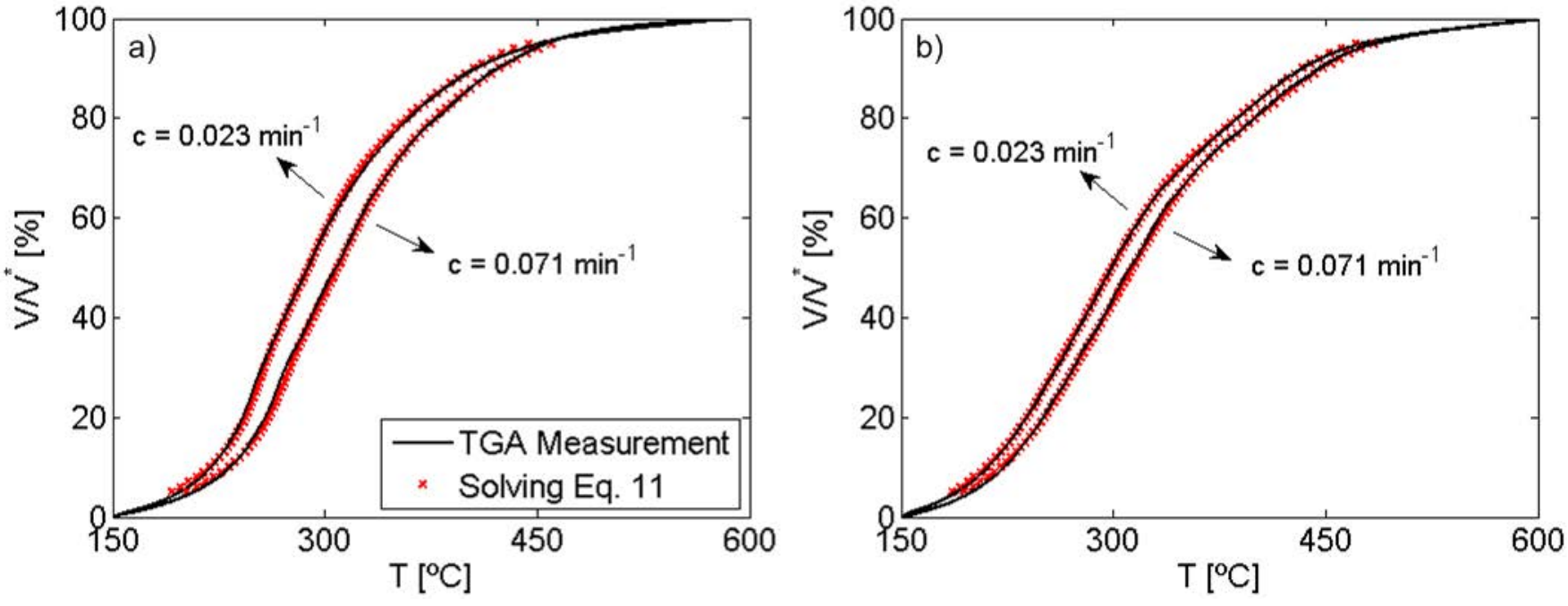

Figure 6: Comparison of experimental and numerical results obtained for the relation between the reacted fraction, V/V^*, and the temperature, T, during the pyrolysis process under exponential temperature increases. a) *C. vulgaris*, b) Sewage sludge.

The deviation between the numerical estimation of the temperature from Eq. 11 and the experimental measurement carried out in the TGA during the pyrolysis of the samples under exponential temperature increases is shown in Figure 7 for total reaction times around 70 and 210 min, depending on the different exponential temperature profiles used. Low deviations of less than 4 °C between the numerically obtained and the experimentally measured temperature are obtained for both the microalgae and the sewage sludge samples for both exponential temperature profiles, in a range of reacted fractions between 20% and 80%, when the pyrolysis process is faster. Higher deviations of less than 9 °C are obtained for lower (<20%) and higher (>80%) values of the reacted fraction, where the linearity of the Arrhenius plot was lower (see Figure 3) and thus the uncertainties associated with the kinetic parameters of the pyrolysis reaction increased (see Figure 5). These low temperature deviations obtained for exponential temperature increases indicate that the activation energy E_a and the pre-exponential factor k_0 shown in Figure 4 for the *C. vulgaris* and the sewage sludge pyrolysis, and the Arrhenius equation (Eq. 11) derived by [34], could be employed to simulate the pyrolysis process occurring in these fuel particles when the Lumped Capacitance Method can be applied.

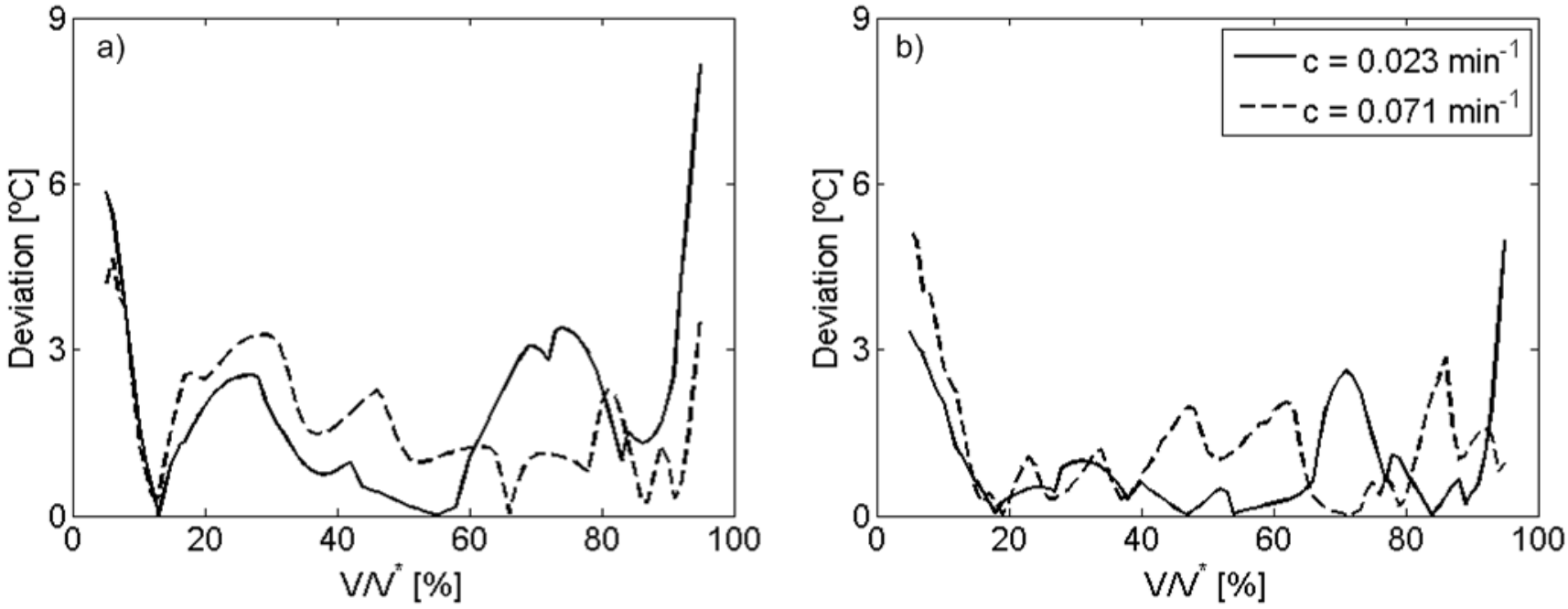

Figure 7: Deviations between the temperature estimated by the Arrhenius equation (Eq. 11) and the temperature measured in TGA for the pyrolysis under exponential temperature increases. a) *C. vulgaris*, b) Sewage sludge.

4.5. Parabolic temperature increases

The parabolic temperature increases programmed in the TGA for the pyrolysis tests of the samples were in the form:

$$T\left[^{\circ}\mathrm{C}\right] = 150 + b \cdot t^{2} \tag{12}$$

Two different values of *b, b = 0.050* ºC·min^{-2} and *b = 0.464* ºC·min^{-2}, were employed during the tests to obtain two different parabolic temperature increases during the pyrolysis measurements in the TGA, these being the limit values studied in [34]. Additionally, [34] obtained the Arrhenius equation derived from the simplified Distributed Activation Energy Model for parabolic temperature increases:

$$\ln\left(\frac{\sqrt{b}}{T^{1.5}}\right) = \ln\left(\frac{k_0 R}{2E_a}\right) + 1.0715 - \frac{E_a}{R}\frac{1}{T} \tag{13}$$

The values of the activation energy E_a and the pre-exponential factor k_0 of the samples, shown in Figure 4, were used to solve Eq. 13, determining the temperature *T* at which each reacted fraction *V/V** occurred. The results of the measurements during the pyrolysis process of the samples in the TGA under parabolic temperature increases are plotted, together with the numerical solution of Eq. 13, in Figure 8. A good agreement between the numerical estimation and the experimental measurements can be observed in Figure 8 both for the *C. vulgaris* and the sewage sludge pyrolysis processes. The pyrolysis processes with the lower value of *b* have a slower temperature rise with a more than 3 times longer reaction time (around 95 min for complete pyrolysis) which results in a higher amount of reacted fraction at lower temperature than

during the pyrolysis processes with the higher value of *b*, which still needs more than 30 min for complete pyrolysis.

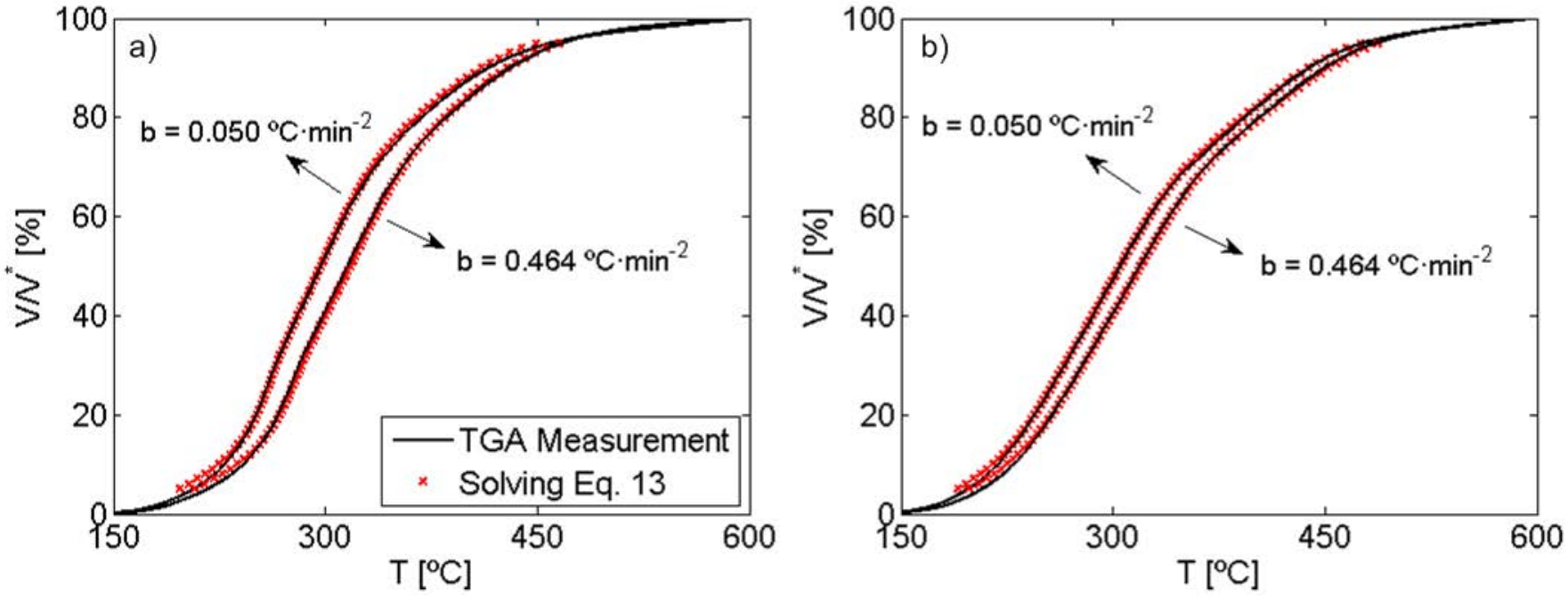

Figure 8: Comparison of experimental and numerical results obtained for the relation between the reacted fraction, *V/V**, and the temperature, *T*, during the pyrolysis process under parabolic temperature increases. a) *C. vulgaris*, b) Sewage sludge.

The deviations between the temperatures estimated solving Eq. 13 and the TGA measurements during the pyrolysis process of the samples under parabolic temperature increases can be observed in Figure 9. The deviations between the numerical and the experimental temperature are again lower than 4 °C for a wide range of reacted fractions, between 20% and 80%. As for the case of the pyrolysis under exponential temperature increases, the temperature deviations for the pyrolysis under parabolic temperature increases are slightly higher for reacted fractions lower than 20% and higher than 80%, where the uncertainties associated with the activation energy and the pre-exponential factor are higher (Figure 5). In view of the low deviations obtained between the numerical and the experimental temperatures, shown in Figure 9, the kinetic parameters of the pyrolysis reaction, E_a and k_0, for the *C. vulgaris* and the sewage sludge shown in Figure 4, and the Arrhenius equation (Eq. 13) derived by [34], could be employed to simulate the pyrolysis process occurring in these fuel particles subjected to parabolic temperature increases.

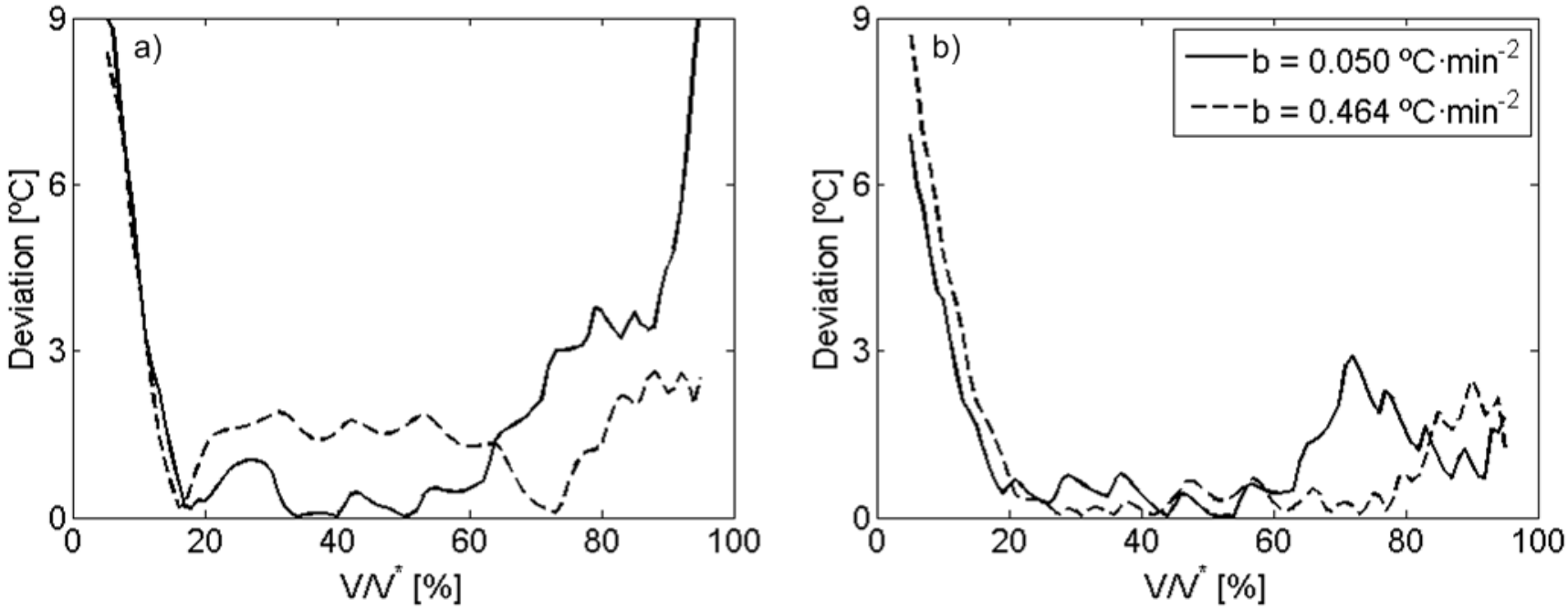

Figure 9: Deviations between the temperature estimated by the Arrhenius equation (Eq. 13) and the temperature measured in TGA for the pyrolysis under parabolic temperature increases. a) *C. vulgaris*, b) Sewage sludge.

5. Conclusions

Non-isothermal thermogravimetric analysis was employed to characterize the pyrolysis of *C. vulgaris* and sewage sludge. The simplified Distributed Activation Energy Model was applied to simulate the pyrolysis of the samples, obtaining the activation energy and the pre-exponential factor of *C. vulgaris* and sewage sludge, together with their associated uncertainties. The activation energies of *C. vulgaris* are in the range of 150 – 250 kJ/mol and its pre-exponential factor varies between 10^{10} and 10^{15} s^{-1}, whereas for the sewage sludge the activation energies range between 200 and 400 kJ/mol and pre-exponential factors vary from 10^{15} to 10^{20} s^{-1}.

Experimental measurements of the pyrolysis process of the samples under exponential and parabolic temperature increases were conducted in the TGA, and the corresponding Arrhenius equations for these temperature increases were solved using the values obtained for the pyrolysis kinetic parameters. The comparison of the experimental and numerical data resulted in excellent agreement, confirming the accuracy of the values reported for E_a and k_0. Thus, the values reported for the activation energy and the pre-exponential factor for the *C. vulgaris* can be employed as reference values in numerical studies of the pyrolysis of this biofuel due to its homogeneity of chemical and biological composition. However, for sewage sludge pyrolysis the situation is quite different due to its variable composition. Therefore, the pyrolysis kinetic parameters obtained for our sewage sludge sample can be only used for modelling the pyrolysis of sewage sludge with a similar composition, or in cases where no better data are available.

Acknowledgments

The authors express their gratitude to the BIOLAB experimental facility and to the “Programa de movilidad de investigadores en centros de investigación extranjeros (Modalidad A)” from the Carlos III University of Madrid (Spain) for the financial support conceded to Antonio Soria for a research stay at the German Aerospace Center DLR (Stuttgart, Germany) during the summer of 2016. The authors also gratefully acknowledge the financial support provided by Fundación Iberdrola under the “VI Programa de Ayudas a la Investigación en Energía y Medioambiente”. Funding by the energy, combustion, and gas turbine technology program (EVG) of Deutsches Zentrum für Luft- und Raumfahrt e. V. (DLR), the German Aerospace Center, is gratefully acknowledged as well as funding by the DLR international collaboration project “Accurate Kinetic Data of Biomass Pyrolysis”.

References

[1] Demirbas A, Demirbas MF. Importance of algae oil as a source of biodiesel. Energ. Convers. Manage. 2011; 52, 163-170.

[2] Fonts I, Azuara M, Gea G, Murillo MBJ. Study of the pyrolysis liquids obtained from different sewage sludge. J. Anal. Appl. Pyrol. 2009; 85, 184-191.

[3] Manara P, Zabaniotou A. Towards sewage sludge based biofuels via thermochemical conversion - A review. Renew. Sust. Energ. Rev. 2012; 16, 2566-2582.

[4] Rulkens W. Sewage Sludge as a Biomass Resource for the Production of Energy: Overview and Assessment of the Various Options. Energ. Fuel. 2008; 22, 9–15.

[5] Fytili D, Zabaniotou A, Utilization of sewage sludge in EU application of old and new methods - A review. Renew. Sust. Energ. Rev. 2008;12, 116−140.

[6] Tran KQ, Bui HH, Chen WH. Distributed activation energy modelling for thermal decomposition of microalgae residues. Chem. Eng. Transactions 2016; 50, 175-180.

[7] Milano J, Ong HC, Masjuki HH, Chong WT, Lam MK, Loh PK, Vellayan V. Microalgae biofuels as an alternative to fossil fuel for power generation. Renew. Sust. Energ. Rev. 2016; 58, 180-197.

[8] Figueira CA, Moreira PF, Giudici R. Thermogravimetric analysis of the gasification of microalgae C. vulgaris. Bioresource Technol. 2015; 198, 717-724.

[9] Marcilla A, Catalá L, García-Quesada JC, Valdés FJ, Hernández MR. A review of thermochemical conversion of microalgae. Renew. Sust. Energ. Rev. 2013; 27, 11-19.

[10] Samolada MC, Zabaniotou AA. Comparative assessment of municipal sewage sludge incineration, gasification and pyrolysis for a sustainable sludge-to-energy management in Greece. Waste Manag. 2014; 34, 411-420.

[11] Coats AW, Redfern JP. Kinetic parameters from thermogravimetric data. Nature 1964; 201, 68-69.

[12] Anca-Couce A, Berger A, Zobel N. How to determine consistent biomass pyrolysis kinetics in a parallel reaction scheme. Fuel 2014; 123, 230-240.

[13] Li Z, Zhao W, Meng B, Liu C, Zhu Q, Zhao G. Kinetic study of corn straw pyrolysis: comparison of two different three-pseudo component models. Bioresource Technol. 2008; 99, 7616–7622.

[14] Lin T, Goos E, Riedel U. A sectional approach for biomass: Modelling the pyrolysis of cellulose. Fuel Process. Technol. 2013; 115, 246-253.

[15] Vand V. A theory of the irreversible electrical resistance changes of metallic films evaporated in vacuum. Proc. Phys. Soc. 1943; 55, 222-246.

[16] Miura K. A new and simple method to estimate f(E) and $k_0(E)$ in the distributed activation energy model from three sets of experimental data. Energ. Fuel. 1995; 9, 302-307.

[17] Miura K, Maki T. A simple method for estimating f(E) and $k_0(E)$ in the distributed activation energy model. Energ. Fuel. 1998; 12, 864-869.

[18] Günes M, Günes SK. Distributed activation energy model parameters of some Turkish coals. Energy Sources Part A - Recovery Utilization and Environmental Effects 2008; 30, 1460-1472.

[19] Várghegyi G, Szabó P, Antal MJ. Kinetics of charcoal devolatilization. Energ. Fuel. 2002; 16, 724-731.

[20] Wanjun T, Cunxin W, Donghua C. Kinetic studies on the pyrolysis of chitin and chitosan. Polym. Degrad. Stabil. 2005; 87, 389-394.

[21] Wang Q, Wang H, Sun B, Bai J, Guan X. Interactions between oil shale and its semi-coke during co-combustion. Fuel 2009; 88, 1520-1529.

[22] Yan JH, Zhu HM, Jiang XG, Chi Y, Cen KF. Analysis of volatile species kinetics during typical medical waste materials pyrolysis using a distributed activation energy model. J. Hazard. Mater. 2009; 162, 646-651.

[23] Soria-Verdugo A, Garcia-Hernando N, Garcia-Gutierrez LM, Ruiz-Rivas U Analysis of biomass and sewage sludge devolatilization using the distributed activation energy model. Energ. Convers. Manage. 2013, 65, 239-244.

[24] Ceylan S, Kazan D. Pyrolysis kinetics and thermal characteristics of microalgae Nannochloropsis oculata and Tetraselmis sp. Bioresource Technol. 2015; 187, 1-5.

[25] Yang X, Zhang R, Fu J, Geng S, Cheng JJ, Sun Y. Pyrolysis kinetic and product analysis of different microalgal biomass by distributed activation energy model and pyrolysis-gas chromatography-mass spectrometry. Bioresource Technol. 2014; 163, 335-342.

[26] Hu S, Jess A, Xu M. Kinetic study of Chinese biomass slow pyrolysis: Comparison of different kinetic models. Fuel 2007; 86, 2778-2788.

[27] Cai J, Liu R. New distributed activation energy model: Numerical solution and application to pyrolysis kinetics of some types of biomass. Bioresource Technol. 2008; 99, 2795-2799.

[28] Cai J, Wu W, Liu R. An overview of distributed activation energy model and its application in the pyrolysis of lignocellulosic biomass. Renew. Sust. Energ. Rev. 2014; 36, 236–246.

[29] Sonobe T, Worasuwannarak N. Kinetic analyses of biomass pyrolysis using the distributed activation energy model. Fuel 2008; 87, 414-421.

[30] Shen DK, Gu S, Jin B, Fang MX. Thermal degradation mechanisms of wood under inert and oxidative environments using DAEM methods. Bioresource Technol. 2011; 102, 2047-2052.

[31] Soria-Verdugo A, Garcia-Gutierrez LM, Blanco-Cano L, Garcia-Gutierrez N, Ruiz-Rivas U. Evaluating the accuracy of the Distributed Activation Energy Model for biomass devolatilization curves obtained at high heating rates. Energ. Convers. Manage. 2014; 86 1045–1049.

[32] Soria-Verdugo A, Goos E, Garcia-Hernando N. Effect of the number of TGA curves employed on the biomass pyrolysis kinetics results obtained using the Distributed Activation Energy Model. Fuel Process. Technol. 2015; 134, 360-371.

[33] Soustelle M. Handbook of Heterogenous Kinetics. John Wiley & Sons. London, 2010.

[34] Soria-Verdugo A, Goos E, Arrieta-Sanagustín J, García-Hernando N. Modeling of the pyrolysis of biomass under parabolic and exponential temperature increases using the Distributed Activation Energy Model. Energ. Convers. Manage. 2016; 118, 223-230.

[35] Mani T, Murugan P, Abedi J, Mahinpey N. Pyrolysis of wheat straw in a thermogravimetric analyzer: effect of particle size and heating rate on devolatilization and estimation of global kinetics. Chem. Eng. Res. Des. 2010; 88, 952-958.

528 [36] Vassilev SV, Vassileva CG. Composition, properties and challenges of algae biomass for biofuel
529 application: An overview. Fuel 2016; 181, 1-33.

530 [37] Bach QV, Chen WH, Lin SC, Sheen HK, Chang JS. Wet torrefaction of microalga Chlorella vulgaris
531 ESP-31 with microwave-assisted heating. Energ. Convers. Manage. 2016; In Press.

532 [38] Ferreira AF, Soares Dias AP, Silva CM, Costa M. Evaluation of thermochemical properties of raw and
533 extracted microalgae. Energy 2015; 92 365-372.

534 [39] Belotti G, de Caprariis B, de Filippis P, Scarsella M, Verdone N. Effect of Chlorella vulgaris growing
535 conditions on bio-oil production via fast pyrolysis. Biomass Bioenerg. 2014; 61, 187-195.

536 [40] Gong X, Zhang B, Zhang Y, Huang Y, Xu M. Investigation on pyrolysis of low lipid microalgae Chlorella
537 vulgaris and Dunaliella salina. Energ. Fuel. 2014; 28, 95-103.

538 [41] López-González D, Fernandez-Lopez M, Valverde JL, Sanchez-Silva L. Kinetic analysis and thermal
539 characterization of the microalgae combustion process by thermal analysis coupled to mass spectrometry.
540 Appl. Energy 2014; 114, 227-237.

541 [42] Rizzo AM, Prussi M, Bettucci L, Libelli IM, Chiaramonti D. Characterization of microalga Chlorella as a fuel
542 and its thermogravimetric behavior. Appl. Energy 2013; 102, 24-31.

543 [43] Chen C, Lu Z, Ma X, Long J, Peng Y, Hu L, Lu Q. Oxy-fuel combustion characteristics and kinetics of
544 microalgae Chlorella vulgaris by thermogravimetric analysis. Bioresour. Technol. 2013; 144; 563–571.

545 [44] Yuan T, Tahmasebi A, Yu J. Comparative study on pyrolysis of lignocellulosic and algal biomass using
546 a thermogravimetric and a fixed-bed reactor. Bioresource Technol. 2015; 175, 333-341.

547 [45] Bresters AR, Coulomb I, Deak B, Matter B, Saabye A, Spinosa L, Utvik AØ, Uhre L, Meozzi P. Sludge
548 Treatment and Disposal - Management Approaches and Experiences. Environmental Issues Series no. 7, 1-
549 53, 1997 ISWA, European Environment Agency.

550 [46] Scott SA, Dennis JS, Davidson JF, Hayhurst AN. Thermogravimetric measurements of the kinetics of
551 pyrolysis of dried sewage sludge. Fuel 2006; 85, 1248–53.

552 [47] Jayaraman K, Gökalp I. Pyrolysis, combustion and gasification characteristics of miscanthus and
553 sewage sludge. Energ. Convers. Manage. 2015, 89, 83-91.

554 [48] Kan T, Strezov V, Evans T. Effect of the Heating Rate on the Thermochemical Behavior and Biofuel
555 Properties of Sewage Sludge Pyrolysis. Energ. Fuel. 2016; 30, 1564-1570.

[49] Thipkhunthod P, Meeyoo V, Rangsunvigit P, Kitiyanan B, Siemanond K, Rirksomboon T. Pyrolytic characteristics of sewage sludge. Chemosphere 2006; 64, 955-962.

[50] Dümpelmann R, Richarz W, Stammbach MR. Kinetic studies of the pyrolysis of sewage sludge by TGA and comparison with fluidized beds. Can. J. Chem. Eng. 1991; 69, 953.-963.

[51] Fan H, He K. Fast Pyrolysis of Sewage Sludge in a Curie-Point Pyrolyzer: The Case of Sludge in the City of Shanghai, China. Energ. Fuel. 2016; 30, 1020-1026.

[52] Magdziarz A, Werle S. Analysis of the combustion and pyrolysis of dried sewage sludge by TGA and MS. Waste Manage. 2014; 34, 174-179.

[53] Jindarom C, Meeyoo V, Rirksomboon T, Rangsunvigit P. Thermochemical decomposition of sewage sludge in CO2 and N2 atmosphere. Chemosphere 2007; 67, 1477–1484.

[54] Calvo LF, Otero M, Jenkins BM, García AI, Morán A. Heating process characteristics and kinetics of sewage sludge in different atmospheres. Thermochim. Acta 2004; 409; 127–135.

[55] Inguanzo M, Domínguez A, Menéndez JA, Blanco CG, Pis JJ. On the pyrolysis of sewage sludge: the influence of pyrolysis conditions on solid, liquid and gas fractions. J. Anal. Appl. Pyrol. 2002; 63, 209-222.

[56] Caballero JA, Front R, Marcilla A, Conesa JA. Characterization of sewage sludges by primary and secondary pyrolysis. J. Anal. Appl. Pyrol. 1997; 40-41, 433-450.

[57] Conesa JA, Marcilla A, Prats D, Rodriguez-Pastor M. Kinteic study of the pyrolysis of sewage sludge. Waste Manage. Res. 1997; 15, 293-305.

[58] Liu G, Song H, Wua J. Thermogravimetric study and kinetic analysis of dried industrial sludge pyrolysis. Waste Manage. 2015; 41, 128–133.

[59] Munir S, Daood SS, Nimmo W, Cunliffe AM, Gibbs BM. Thermal analysis and devolatilization kinetics of cotton stalk, sugar cane bagasse and shea meal under nitrogen and air atmosphere, Bioresource Technol. 2009; 100, 1413-1418.

[60] Tonbul Y, Saydut A, Yurdako K, Hamamci C. A kinetic investigation on the pyrolysis of Seguruk asphaltite. J. Therm. Anal. Calorim. 2009; 95, 197-202.

[61] Chen C, Ma X, He Y. Co-pyrolysis characteristics of microalgae Chlorella vulgaris and coal through TGA. Bioresource Technol. 2012; 117, 264-273.

[62] Maurya R, Ghosh T, Saravaia H, Paliwal C, Ghosh A, Mishra S. Non-isothermal pyrolysis of de-oiled microalgal biomass kinetics and evolved gas analysis. Bioresource Technol. 2016; 221, 251-261.

585 [63] Hu M, Chen Z, Guo D, Liu C, Xiao B, Hu Z, Liu S. Thermogravimetric study in pyrolysis kinetics of
586 Chlorella pyrenoidosa and bloom-forming cyanobacteria. Bioresource Technol. 2015; 177, 41-50.

587 [64] Zhao B, Wang X, Yang X. Co-pyrolysis characteristics of microalgae Isochrysis and Chlorella: Kinetics,
588 biocrude yield and interaction. Bioresource Technol. 2015; 198, 332-339.

589 [65] Figueira CE, Moreira Jr PF, Giudicini R. Thermogravimetric analysis of the gasification of microalgae
590 Chlorella vulgaris. Bioresource Technol. 2015; 198, 717-724.

591 [66] Kassim MA, Kirtania K, de la Cruz D, Cura N, Srivalsa SC, Bhattacharya S. Thermogravimetric analysis
592 and kinetic characterization of lipid-extracted Tetraselmis suecica and Chlorella sp. Algal Res. 2014; 6, 39-
593 45.

594 [67] Lin Y, Liao Y, Yu Z, Fang S, Lin Y, Fan Y, Peng X, Ma X. Co-pyrolysis kinetics of sewage sludge and oil
595 shale thermal decomposition using TGA-FTIR analysis. Energ. Convers. Manage. 2016, 118, 345-352.

596 [68] Huang L, Liu J, He Y, Sun S, Chen J, Sun J, Chang K, Kuo J, Ning X. Thermodynamics and kinetics
597 parameters of co-combustion between sewage sludge and water hyacinth in CO_2/O_2 atmosphere as
598 biomass to solid biofuel. Bioresource Technol. 2016; 218, 631-642.

599 [69] Wang X, Zhao B, Yang X. Co-pyrolysis of microalgae and sewage sludge: biocrude assessment and
600 char yield prediction. Energ. Convers. Manage. 2016, 117, 326-334.

601 [70] Urych B, Smolinski A. Kinetics of sewage sludge pyrolysis and air gasification of its chars. Energ. Fuel.
602 2016; 30, 4869-4878.

List of figures

List of tables